

Adiabatic-Passage Based Parameter Setting Method for Quantum Approximate Optimization Algorithm on 3-SAT Problem

Mingyou Wu¹, Zhihao Liu^{1,2}, and Hanwu Chen^{1,2}

¹School of Computer Science and Engineering, Southeast University, Nanjing 211189, China

²Key Laboratory of Computer Network and Information Integration (Southeast University), Ministry of Education, Nanjing, 211189, China

December 4, 2023

Abstract

The quantum approximate optimization algorithm (QAOA) shows great computational potential on combinatorial optimization problems. It is a promising algorithm on near-term quantum devices, but one of the difficulty in application of QAOA is the complexity of parameter setting. In this paper, an adiabatic-passage based parameter setting method is proposed and applied to 3-SAT. And in simulation, the optimization cost is significantly reduced, approximately between sublinear to logarithmic on the depth p of QAOA. The efficiency of this method mainly stems from two aspects, one is the problem-oriented preprocessing of Hamiltonian, and the other is the parameter space adjustment based on the continuity of adiabatic passage. Firstly, a random model for 3-SAT is provided and the problem Hamiltonian of this model is designed as a random matrix. Based on the statistical property of randomized Hamiltonian, the Hamiltonian of QAOA is preprocessed and the parameter setting is separated from the overall property of the problem. As a result, a good initialization can be obtained. Secondly, the optimal adiabatic passage is introduced and actually, the QAOA can be regarded as the parameterization of adiabatic passage and the optimization as the search of the optimal adiabatic passage. Based on this, the adiabatic passage is parameterized as another parameter space with better continuity and the adiabatic-passage based parameter setting method is proposed.

1 Introduction

Quantum computation [1] is an emerging computational model that follows the quantum mechanics and uses quantum systems as basic computing units. Like the digital computer, the different basic states of these units are encoded into binary data of $|0\rangle$ or $|1\rangle$, named qubits. However, in quantum mechanics, the state of quantum system can not only be in computational base, but also in any superposition of these bases. This allows high parallelism in quantum computing that at most $N = 2^n$ values can be processed simultaneously, where n is the number of qubits. This parallelism has restrictions like the measurement of quantum state [1], but by properly design the algorithm, speedup is shown in various of problems. The prime factorization algorithm proposed by Shor in 1994 is a well-known quantum algorithm with complexity $O(\log^3(N))$ [2]. And in 1997, Grover presented a search algorithm on unstructured databases that has a quadratic acceleration as compared to the classical algorithm [3]. The HHL algorithm proposed by Harrow, Hassidim and Lloyd in 2009 solves linear equations in $O(k^2 \log(N))$ time [4].

These quantum algorithms exhibit provable exponential or polynomial accelerations compared with existing classical algorithms. While in the present stage, only noisy intermediate-scale quantum (NISQ) devices are available, and because of noisy, this is insufficient to show quantum advantage over classical computers using such algorithms [5]. In NISQ era, it is essential to develop proper noisy-tolerate quantum algorithms

and one of the emerging concern is the hybrid quantum-classical algorithms that adopts parameterized quantum circuits and adjusts the parameters by classical optimization [6]. And the most representative are the variational quantum eigensolver (VQE) [9, 10] for quantum chemistry calculations, quantum neural networks (QNN) [8, 7] for machine learning tasks, and the quantum approximate optimization algorithm (QAOA) [11]. QAOA is a promising approach to be implemented on NISQ device [12, 13] and shows great computational potential on combinatorial optimization. And it is discussed a lot in many aspects. In 2017, a near-optimal quantum circuit [14] is presented by applying the Grover Hamiltonian as problem Hamiltonian to QAOA for the Grover’s unstructured search [3] and it shows that QAOA is at least as efficient as the Grover search. Actually, for some special instances, theoretical results can be obtained [15, 18, 16, 17], and some theoretical analysis is presented to reveal the potential computational power of QAOA [19, 20, 21]. Besides, several variations of QAOA like [23, 24, 22] are proposed to specialize in different types of problem. Still, if without proper strategy, the complexity of parameter setting increases exponentially with the increasing of depth p because of the curse of dimensionality.

It is an essential thesis to reduce the cost of parameter setting of QAOA. Similar to quantum adiabatic algorithm (QAA) [25, 26] and VQE, QAOA defines the problem Hamiltonian H_C and evolve the quantum state to the eigenstate with the maximal (or minimal) eigenvalue of H_C . But differently, QAOA alternately applies the problem Hamiltonian H_C and mix Hamiltonian H_B for p times, and the evolution time is adopted as parameters γ and β . Generally, for an NP-complete combinatorial optimization problem of scale n , it is hard to restrict the depth of QAOA to be a constant or logarithm of n . And if the depth $p = O(\text{Poly}(n))$, the polynomial number of parameters would result in exponential complexity for parameters adjusting. To apply QAOA, different kinds of techniques are applied to reduce the cost of parameter setting, including classical optimization [27], machine learning algorithm [28, 31, 29, 30] and some other heuristic strategies [32, 36, 33, 34, 35]. The heuristic strategy in [32] is one of the most representative that reduces the optimization cost to approximately polynomial on p . And in this paper, an adiabatic-passage based parameter setting method is proposed and it further reduces the cost to approximately between sublinear to logarithmic on p .

In this work, an adiabatic-passage based parameter setting method for QAOA is proposed and it is applied to 3-SAT. The method starts with analysis of the statistical property of problem. For the 3-SAT decision problem, it is reduced a satisfiable 3-SAT optimization version, and a random satisfiable k-SAT model is built similar to the random k-SAT model [37]. The randomized Hamiltonian of this model can be designed and based on this, the statistical property of problem Hamiltonian of the random instances can be obtained and the preprocessing on Hamiltonian can be conducted. Moreover, based on the preprocessing, a good initialization inspired by QAA can be obtained that presets all these $2p$ parameters at the start of QAOA. Furthermore, this initialization can be modified as a linear-varying parameter adjusting method like the INTERP heuristic strategy in [32], and it is an intermediate version of the method.

Besides, to setting the full parameters, the optimal adiabatic passage (AP) is introduced. Actually, the optimal adiabatic passage can be proved to be continuous, and the QAOA can be regarded as the parameterization of adiabatic passage and the optimization as the search of the optimal adiabatic passage. Based on this, the continuity between parameters is discussed in detail and another parameter space with better continuity and interpretability is presented. And furthermore, to better utilize this continuity, the adiabatic-passage based parameter setting method is proposed. Comparisons are conducted with the heuristic strategies in [32], specifically, the QAA-inspired method with INTERP and the AP-based method with FOURIER. In simulation on 3-SAT, INTERP requires $O(p)$ optimization costs, while the QAA-inspired method only needs constant costs with the increase of p . In addition, the cost of FOURIER approximately follows a $O(p^2)$ grows, while the AP-based method further reduces the cost, approximately between sublinear to logarithmic on p .

The remainder of this paper is organized as follows. Section 2 discusses the statistical property of random k-SAT model and based on this, the Hamiltonian of QAOA is preprocessed. In Section 3, a QAA-inspired parameter initialization is firstly introduced based on the preprocessing and it can be simply modified to a QAA-inspired parameter adjusting method with linear parameters. Furthermore, the continuity of full parameters is discussed based on the analysis of optimal adiabatic passage, and another parameter space

with better continuity is introduced. Based on this, the adiabatic-passage based parameter setting method is proposed. Section 4 shows the performance on 3-SAT and compares these methods with the heuristic strategies proposed in [32]. Finally, Section 5 concludes this paper and discusses the remaining problems and further researches.

2 Hamiltonian preprocessing of QAOA based on random k-SAT model

Combinatorial optimization is a widely concerned problem and it is applied in many areas[38]. Combinatorial optimization problem generally has a specific goal function $C(x)$ and it tries to find an optimal goal t from a finite set $\{x\}$ that maximizes $C(x)$. x can be encoded in an n -bit binary string and n is called the scale of problem. The quantum approximate optimization algorithm mainly tackles these combinatorial optimization problems. It defines the problem Hamiltonian as $H_C|x\rangle = C(x)|x\rangle$ and aims to find the target state $|t\rangle$ with maximal energy by a layered variational quantum circuit, written as

$$|\boldsymbol{\gamma}, \boldsymbol{\beta}\rangle = \prod_{d=1}^p (e^{-i\beta_d H_B} e^{-i\gamma_d H_C} |+\rangle^{\otimes n}), \quad (1)$$

where H_B is mix Hamiltonian $\sum_j \sigma_z^{(j)}$ and p is the layer (or depth). $(\boldsymbol{\gamma}, \boldsymbol{\beta})$ is the variational parameter that tries to maximize the expectation $\langle H_C \rangle = \langle \boldsymbol{\gamma}, \boldsymbol{\beta} | H_C | \boldsymbol{\gamma}, \boldsymbol{\beta} \rangle$.

The Boolean satisfiability (SAT) is a well-known NP-complete problem that determines whether there exists an interpretation satisfying a given Boolean formula. The k-SAT problem restricts the Boolean formula in conjunctive normal form, where each clause is limited to at most k literals and this paper further limits to only k literals. The NP-completeness would be maintained as long as $k \geq 3$. This SAT decision problem can be reduced to an optimization version by designing the goal function as $C(x) = \sum_{\alpha} C_{\alpha}(x)$, where α is the clause and $C_{\alpha}(x)$ is the characteristic function of α that if α is satisfied by x , $C(x) = 1$, otherwise, $C(x) = 0$. The satisfiability can be determined by checking the optima t .

The k-SAT decision problem can be further reduced to a satisfiable k-SAT optimization problem. Dividing the full set U of k-SAT to two subset, U_s for all satisfiable instances and U_u for the unsatisfiable, the satisfiable k-SAT optimization problem only considers instance $I_s \in U_s$ and requires the optimal t that maximizes $C(x)$.

Lemma 1. *The k-SAT decision problem can be reduced to the satisfiable k-SAT optimization problem in polynomial time.*

Proof. If given an algorithm A that solves the satisfiable k-SAT optimization problem, the target t of any instance $I_s \in U_s$ can be find in time $O(f(n))$. Design another algorithm A' that A' accepts all instance $I \in U$ and processes I by A . When running time exceeding $O(f(n))$, algorithm terminates and outputs random result. For any I , A' halts in time $O(f(n))$ and output result x . If $I \in U_s$, x should be the interpretation t and is satisfiable by the Boolean formula, otherwise, x is random value and necessarily unsatisfiable. With verification, the satisfiability can be determined. The verification cost would not exceed $O(f(n))$ and the whole complexity is also $O(f(n))$. \square

Typically, the random k -SAT model $F(n, m, k)$ is widely used in the research of SAT problem [37], and because of the reduction in Lemma 1, it can be further modified as random model only on U_s . $F(n, m, k)$ generates an k -SAT instance of scale n by selecting m clauses uniformly, independently and with replacement among all $2^k C_n^k$ clauses. And two kinds of random model on U_s are provided. $F_s(n, m, k)$ is a natural derivation from $F(n, m, k)$ that only selects clauses as long as the satisfiability is maintained. However, $F_s(n, m, k)$ is hard to analyze theoretically because the optional clause set changes with m . Another random model $F_f(n, m, k)$ is proposed as an approximation of $F_s(n, m, k)$ that randomly provides a pre-fix interpretation t_0 and only selects clauses satisfied by t_0 . If considering the generating process as tree, the difference of these three random model can be presented in Figure 1.

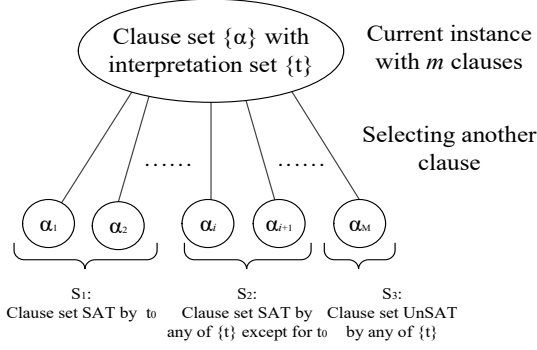


Figure 1: The process of selecting a clause when generating a random k-SAT instance. Suppose $I \in \mathcal{U}_s$ and has interpretation set t . When selecting the next clause, $F(n, m, k)$ randomly selects any clause in $S_1 + S_2 + S_3$ while $F_s(n, m, k)$ selects clause that is satisfiable for any $t \in \mathcal{t}$, namely, $\alpha \in S_1 + S_2$. And $F_f(n, m, k)$ only select clause in S_1 . When $\{t\} = \{t_0\}$, $F_s(n, m, k)$ consists with $F_f(n, m, k)$ and would converges to $F_f(n, m, k)$ with the increase of m .

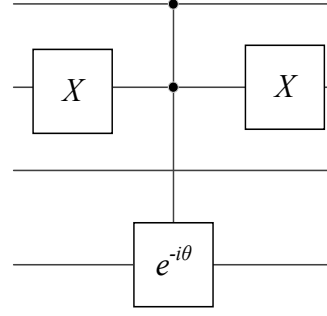


Figure 2: An example of quantum circuit for $e^{i\theta H_\alpha}$ when $\alpha = \neg x_1 \vee x_2 \vee \neg x_4$. This clause can be denoted as $\alpha = (-1, 2, -4)$, and $H_\alpha = -p_{\bar{\alpha}}$. Therefore, the evolution $e^{i\theta H_\alpha} = e^{-i\theta p_{\bar{\alpha}}}$. $\bar{\alpha} = (1, -2, 4)$, and this means the 1-st, 2-rd and 4-th qubits are occupied and an extra pair of X gate on the 2-rd qubit. Here the 4-th qubit is controlled, but the controlled qubit can be any of the involved qubits and the rest are control qubits.

Another kind of decomposition for H_C of k-SAT is introduced. Generally, the diagonal H_C can always be decomposed by the Walsh operator [39] and for k-SAT, can further decomposed into the form of Ising model [40]. Here, to assist the analysis of the statistical properties of H_C , another problem-oriented operator is provided. A Boolean conjunctive $c = (\neg)x_{c_1} \wedge (\neg)x_{c_2} \wedge \dots \wedge (\neg)x_{c_k}$ can be denoted as $c = (\pm c_1, \pm c_2, \dots, \pm c_k)$, where $+c_t$ stands for x_{c_t} and $-c_t$ for $\neg x_{c_t}$. The problem Hamiltonian of c can be written as

$$p_c = P_{\pm}^{(c_1)} \otimes P_{\pm}^{(c_2)} \otimes \dots \otimes P_{\pm}^{(c_k)}, \quad (2)$$

where $P_{\pm}^{(c_t)}$ is P_{\pm} on the c_t -th bit, and $P_+ = |1\rangle\langle 1|$, $P_- = |0\rangle\langle 0|$. For k-SAT, every clause α has the form as $\alpha = (\neg)a_{c_1} \vee (\neg)a_{c_2} \vee \dots \vee (\neg)a_{c_k}$. If also denoting α as $(\pm a_1, \pm a_2, \dots, \pm a_k)$, $H_\alpha = -p_{\bar{\alpha}}$, where $\bar{\alpha} = (\mp a_1, \mp a_2, \dots, \mp a_k)$, and the problem Hamiltonian of k-SAT can be written as

$$H_C = - \sum_{\alpha} p_{\bar{\alpha}}. \quad (3)$$

This Hamiltonian can reduce to Ising model by bringing in $P_{\pm} = \frac{1}{2}(I \mp \sigma_z)$ [40]. The evolution $e^{i\theta H_\alpha}$ is actually k-control phase gate and the circuit complexity is $O(k)$ [41]. In Figure 2, an example is presented.

Based on the random model and decomposition with P operator, the problem Hamiltonian H_C can be analyzed statistically. Considering the problem Hamiltonian of random model $F_f(n, m, k)$ during selecting clauses, because every α is randomly selected, the diagonal matrix H_α can be regarded as a random vector and its eigenvalue $E_{\alpha,x}$ at $|x\rangle$ is random variable. $F_f(n, m, k)$ only selects clause satisfiable by t . Based on this, the mean of $E_{\alpha,x}$ can be obtained as

$$\mu_{k,x} = \frac{2^k - 2}{2^k - 1} + \frac{C_l^k}{(2^k - 1)C_n^k} \leq 1, \quad (4)$$

and the variance is

$$\sigma_{k,x}^2 = (1 - \mu_{k,x})^2 \mu_{k,x} + \frac{\mu_{k,x}^2 (C_n^k - C_l^k)}{(2^k - 1)C_n^k} \leq \frac{1}{2^k - 1}, \quad (5)$$

where $l = n - d_H(x, t)$ and $d_H(x, t)$ is the Hamming distance between x and t . Denote the eigenvalue of H_C as $\mathcal{E}_{k,x} = \sum_{\alpha} E_{\alpha,x}$. For every α , it is selected independently for the same clause set, so $E_{\alpha,x}$ is a sequence of i.i.d. random variables. Based on the central limit theorem, $\mathcal{E}_{k,x}/m$ approximately satisfies the normal distribution that

$$\sqrt{m} \left(\frac{1}{m} \mathcal{E}_{k,x} - \mu_{k,x} \right) \sim N(0, \sigma_{k,x}^2). \quad (6)$$

Obviously, the magnitude of eigenvalue of H_C is $O(m)$, while for the mix Hamiltonian $H_B = \sum_j \sigma_z^{(j)}$, the magnitude of eigenvalue is $O(n)$. For k-SAT problem, the number of clause m can achieve $O(n^k)$ at most. This situation means a significant difference in the energy between H_C and H_B . Even through this difference can be cancelled by adjusting γ and β , but the magnitude difference of parameters would also result in difficulty when optimization. Therefore, a preprocessing can be applied to (approximately) normalize these two Hamiltonian, that is, reducing the maximal energy difference (gap between the maximal and minimal energy) to 1.

The maximal energy difference of H_B is easy to obtain as $2n$, but H_C is undetermined. Moreover, even through H_C is given, it is exponential hard to calculate the maximal energy difference G_0 . But based on the analysis of problem Hamiltonian of random k-SAT, G_0 can be estimated. Based on Eq. (6), the vast majority of eigenvalue $\mathcal{E}_{k,x}$ should satisfy

$$\mu_{k,x} - \frac{c_0}{\sqrt{m(2^k - 1)}} \leq \frac{1}{m} \mathcal{E}_{k,x} \leq \mu_{k,x} + \frac{c_0}{\sqrt{m(2^k - 1)}}. \quad (7)$$

where c_0 is a constant no less than 3. An estimation of G_0 can be obtained by the maximal energy difference of the majority of eigenvalue as

$$\frac{1}{m} G_0 \approx \max \left\{ \mu_{k,x} + \frac{c_0}{\sqrt{m(2^k - 1)}} \right\} - \min \left\{ \mu_{k,x} - \frac{c_0}{\sqrt{m(2^k - 1)}} \right\}, \quad (8)$$

and this estimation should be an approximate lower bound. Noting that $\max\{\mu_{k,x}\} = 1$ and $\mu_{k,x} + c_0/\sqrt{m(2^k - 1)}$ cannot exceed 1, the estimation G_E can be obtained as

$$\frac{1}{m} G_E = \frac{1}{2^k - 1} + \frac{c_0}{\sqrt{m(2^k - 1)}}, \quad (9)$$

This estimation is based on $F_f(n, m, k)$, and because of the similarity between $F_s(n, m, k)$ and $F_f(n, m, k)$, it can also act as an estimation for $F_s(n, m, k)$. A experiment is conducted to compare this estimation G_E with the real G_0 of $F_s(n, m, k)$, and the result is presented in Figure 3. The simulation result shows that this estimation also works for $F_s(n, m, k)$ and therefore, the Hamiltonian can be normalized as

$$\bar{H}_B = \frac{H_B}{2n}, \bar{H}_C = \frac{H_C}{G_E}. \quad (10)$$

3 Parameter setting method

3.1 QAA-inspired parameter initialization

Quantum approximate optimization algorithm is inspired by the Trotterization of quantum adiabatic evolution, and also has a similar form with the Trotterization of QAA. QAA is based on the adiabatic theorem [42] to evolve the quantum state from the ground state of the initial system Hamiltonian $H(0)$ to that of the final $H(T)$. Similar to QAOA, the problem Hamiltonian is defined and the system Hamiltonian is designed as

$$H(t) = \left(1 - \frac{t}{T}\right) H_B + \frac{t}{T} H_C, \quad (11)$$

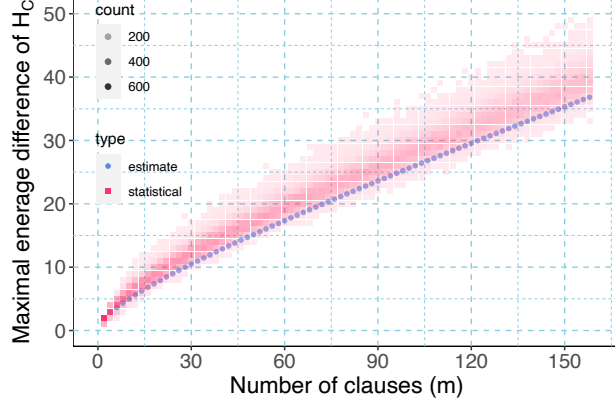


Figure 3: The comparative results of G_0 between the estimation G_E and the statistical result of 1000 instances of $F_s(20, m, 3)$ with different m . The blue round point shows the estimation. The red square points stand for the statistical value and the shades of color represent the count. This estimation approximately describes the low bound and is very close to these darkest square points.

where $0 \leq t \leq T$. In simulation, the time-dependent Hamiltonians $H(t)$ can be approximately Trotterized as a sequence of time-independent Hamiltonians by a small enough Δt . Denoting $p = T/\Delta t$, the evolution of $H(t)$ can be approximately simulated by iterations of evolutions

$$e^{iH(d\Delta t)} \approx e^{-i(1-\frac{d\Delta t}{T})H_B\Delta t} e^{-i\frac{d\Delta t}{T}H_C\Delta t}. \quad (12)$$

This evolution just takes the form of QAOA and the only difference is the parameterized evolution time.

Therefore, it is a straightforward consideration to initialize the parameters based on QAA, that is, adopts a linearly varied $H(t)$. Combined with the normalization of Hamiltonian in Eq. (10), the system Hamiltonian should take the form of

$$\bar{H}(t) = \frac{t}{T} f_\gamma \bar{H}_C + \frac{T-t}{T} f_\beta \bar{H}_B \quad (13)$$

with the best consideration to the degree of freedom, where f_γ and f_β describe the intensity of problem and mix Hamiltonian in evolution. After normalization, the energy of \bar{H}_B and \bar{H}_C should be in the same order of magnitude. Heuristically, the magnitude of f_γ and f_β should also be similar, that is, f_γ probably has a similar value with f_β . Therefore, the intensity of f_γ and f_β can be extracted, and the evolution of QAOA can be regarded as the Trotterization of evolution of Hamiltonian

$$\bar{H}(\theta, t) = \frac{t}{T} \sin \theta \bar{H}_C + \frac{(T-t)}{T} \cos \theta \bar{H}_B \quad (14)$$

with $T = 2p\rho\pi$, and the discretization interval $\Delta t = 2\rho\pi$. In the form of QAOA, with depth of p , the parameters (γ, β) can be written as

$$\gamma_d = \frac{2d\pi}{(p+1)} \rho \sin \theta, \beta_d = \frac{2(p-d+1)\pi}{(p+1)} \rho \cos \theta. \quad (15)$$

Here using $p+1$ is to avoid boundary situation when γ_d or β_d become 0.

The initialization of $2p$ parameters of QAOA is reduced to initialize θ and ρ . θ parameterizes the relative intensity ratio between \bar{H}_C and \bar{H}_B , and because of the normalization of the Hamiltonian, it can be initialized as $\theta = \pi/4$. ρ describes the discretization width of QAA, and also the evolution time of each layer of QAOA. There is no prior knowledge about the expectation of ρ , but it has a natural initialization without demerit that $\rho = \sqrt{2}$ and the reason is as follows. In QAOA, the only problem-related operator is H_C and the evolution $e^{-i\gamma H_C}$ is actually phase shifts $e^{-i\gamma C(x)}$ on every computational basis $|x\rangle$. That is, the target is

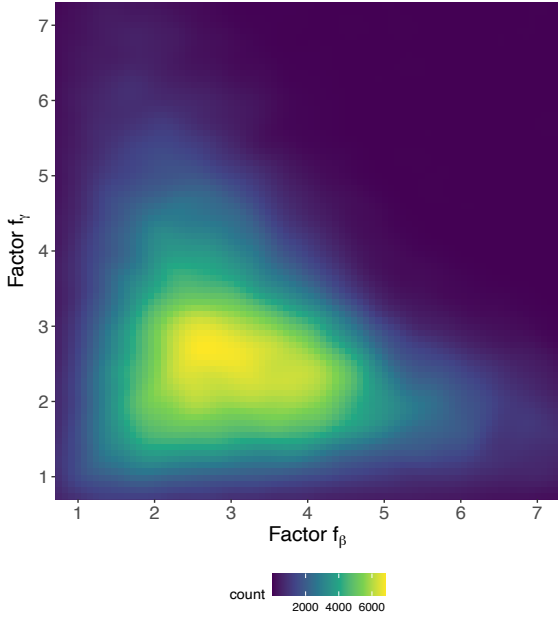


Figure 4: The distribution of the count of obtaining the target state when measurement. For each pair of (f_γ, f_β) , the final state is measured for 10000 times. This simulation is conducted on a random instance in $F_s(12, m, 3)$. To display the effect of normalization, H_C is normalized by its real G_0 . Besides, it implies in [43] that the depth of QAOA should not exceed $O \log(N)$ on NISQ device, so in this paper, the depth p is generally fixed as n .

distinguished by the phase shifts. To best distinguish the target t , $e^{-i\gamma C(t)}$ should be different from the others. And because of the periodicity of phase, a basic consideration is to restrict the range of $\gamma C(x)$ to $[0, 2\pi)$ and for normalized \bar{H}_C , f_γ can be initialize as 1 and $\rho = \sqrt{2}$.

Simulation is conducted to verify this initialization. For a random instance in $F_s(12, m, 3)$, the probability of the target state with different f_γ and f_β is shown in Figure 4. The simulation result shows around the axis $f_\gamma = f_\beta$, the probability increases the fastest and soon reaches the optimum, while if it deviates from this axis, the greater the deviation, the slower the growth rate and the distance from the optimum. Besides, when (f_γ, f_β) crosses a threshold, the probability significantly decreases and it implies the effectiveness of Hamiltonian normalization in parameter optimization.

Although $\rho = \sqrt{2}$ is a feasible initialization, a small ρ means a small evolution time for the specific interval of evolution. In QAOA, the depth p is generally insufficient, and therefore, a reasonable larger ρ means more evolution time and would have better performance as shown in Figure 4. In fact, the random k-SAT model implies that ρ might also has some expectation like θ , but cannot be directly obtained by analysis. Here, another simulation is conducted on 100 random instance in $F_s(n, m, 3)$ with $n = 8, 12, 16, 20$ to analyze the optimal ρ , and the optimized (θ, ρ) are plotted in Figure 5 in polar coordinate system. The result shows that not only the optimal θ is distributed around a certain value, but also ρ . Unlike $\bar{\theta}$ seems to be constant, $\bar{\rho}$ varies with (n, m) and hard to analytical obtain. Therefore, a empirical value $t_0 \geq 1$ can be estimated by experiment on a small set of instances in $F_s(n, m, 3)$ and be used in initialization that $\rho = \sqrt{2}t_0$.

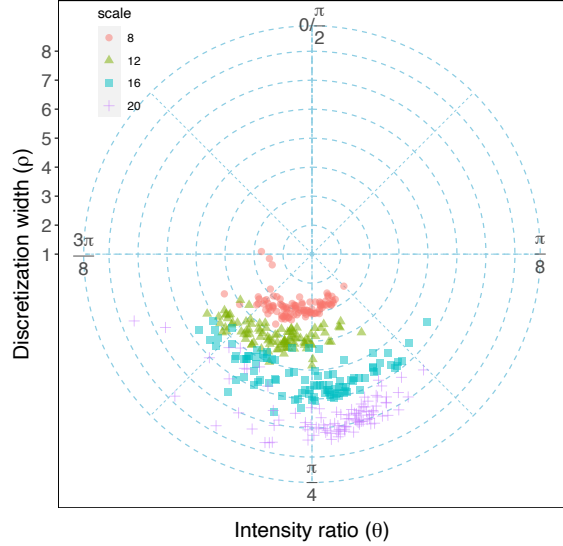


Figure 5: The distribution of optimal (θ, ρ) for different instances of $F_s(n, m, 3)$ in polar coordinate system. And for different scales $n = 8, 12, 16, 20$, the results are plotted in different colors and shapes, respectively are red round, green triangle, blue square and purple cross. The optimal θ generally distributes around $\theta = \pi/4$ and ρ also seems to gather near a certain value. Three idealized conditions are used as follows: first, the problem Hamiltonian H_C is normalized by its accurate G_0 ; second, the optimization aim is to maximize the probability of target state; third, the exhaustive searching is used to find the optimal parameters.

Algorithm 1 QAA-inspired parameter initialization method

Require:

- The cost function $C(x)$ (also the H_C) and the scale n ;
- Proper model for this kind of problem F ;
- Given depth p of QAOA;

Ensure:

- The initial parameters (γ, β) for every depth of QAOA;
 - The normalized Hamiltonians \bar{H}_C and \bar{H}_B ;
 - 1. Estimate the maximal energy difference G_E of H_C based on F ;
 - 2. Normalize the Hamiltonians that $\bar{H}_C \leftarrow H_C/G_E$ and $\bar{H}_B \leftarrow H_B/2n$;
 - 3. Give the empirical value $t_0 \geq 1$ based on F , otherwise, $t_0 \leftarrow 1$;
 - 4. Set initial parameters $\gamma_d \leftarrow \frac{2t_0 d \pi}{p+1}$, $\beta_d \leftarrow \frac{2t_0(p+1-d)\pi}{p+1}$, and the evolution is $\prod_{d=1}^p e^{-i\beta_d \bar{H}_B} e^{-i\gamma_d \bar{H}_C}$.
-

Based on the above analysis, a QAA-inspired parameter initialization is presented in Algorithm 1. The first and second step of this method try to normalize the Hamiltonian H_C and H_B . And the third step tries to find a proper evolution time t_0 for each iteration of QAOA and it is an initialization for ρ . Finally, in the the fourth step, a mapping is build to initialize these $2p$ parameters of QAOA from $\theta = \pi/4$ and $\rho = \sqrt{2}t_0$. In fact, this initialization method can be modified to a QAA-inspired parameter adjusting method by optimizing $\langle H_C \rangle$ by adjusting θ and ρ . And this is suitable for scenario that limits the optimization costs and no need to optimize all parameters of QAOA.

3.2 Adiabatic-passage based parameter setting method

QAA-based initialization method can easily set these $2p$ parameters, but cannot make the full use the computational potential of the circuit. In fact, QAA derives from adiabatic quantum computation [25, 26, 42] with system Hamiltonian of

$$H(s) = sH(s) + (1 - s)H(s), \quad (16)$$

where $0 \leq s \leq 1$. The evolution time of $H(s)$ should satisfies

$$T \gg \frac{\varepsilon_0}{g_0^2}. \quad (17)$$

g_0 is the minimum of energy gap between the minimum and subminimum eigenstate $\psi_1(s)$ and $\psi_2(s)$ of $H(s)$. Denoting $g(s)$ as the gap between $\psi_1(s)$ and $\psi_2(s)$, $g_0 = \min_s g(s)$. And ε_0 is determined by the maximum of derivative of $H(s)$ that

$$\varepsilon_0 = \max_s \left\langle \psi_1(s) \left| \frac{d}{ds} H(s) \right| \psi_2(s) \right\rangle. \quad (18)$$

In simulation, the mapping from $s \in [0, 1]$ to $t \in [0, T]$ should be determined and QAA simply adopts a linear varying $H(t)$. Therefore, $\frac{d}{dt} H(t)$ is invariant and the evolution time of QAA is only quadratic inverse correlated with g_0 .

The inefficiency of QAA in utilization of quantum circuit can be shown by a simple modification as a segmented QAA. The segmented QAA divides the whole evolution to several segment as $H(s_1), H(s_2), \dots, H(s_l)$, and every segment $[H(s_i), H(s_{i+1}))$ applies QAA independently. Now, the minimal gap of this segment is only determined by $[s_i, s_{i+1})$, other than the global minimum g_0 . Because not every segment has a minimal gap as g_0 , the required evolution in this segment would reduce. As a result, the whole required time is reduced and so is the depth of circuit. A simulation of segmented QAA is conducted and QAA of each segment is optimized with the less evolution time as long as the probability of aimed state is more than 99%. The gap $g(s)$ and the evolution time are presented in Figure 6.

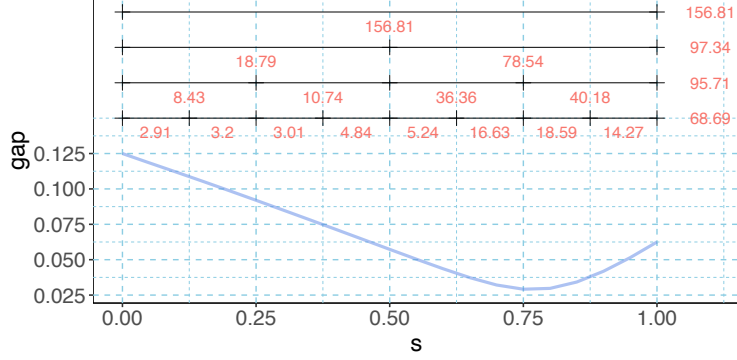


Figure 6: The simulation result of segmented QAA on random instance in $F_s(n, m, 3)$. In the lower part of figure, the blue solid line shows the varying of the gap. The upper part displays different kinds of even segmentation of $H(t)$ in black lines and crosses, no segmentation, 2, 4, 8-segmented, respectively. The evolution time of each interval is plotted in red number below each interval, and the total evolution time is displayed in the far right. For the interval with a larger gap, the required time is much less and as a result, the total evolution time is significantly reduced with more segments. Besides, if the segmentation is not even, but flexible and optimized, the total evolution time can be further reduced.

If the number of segments is large, every segment can be small enough. For a small segment $[s_j, s_j + \Delta s)$, the least required evolution time should satisfy $T_j \sim \varepsilon(s_j)g^{-2}(s_j)$. When $\Delta s \rightarrow 0$, the required time of the optimal evolution should satisfy

$$T = O\left(\int_0^1 \varepsilon(s)g_0^{-2}(s)ds\right). \quad (19)$$

To describe this optimal evolution, the ‘‘adiabatic passage’’ is introduced. Adiabatic evolution is based on adiabatic theory and driven by the Schrödinger equation. For a specific problem, the system Hamiltonian $H(t)$ is not unique, but always follow the form as

$$H(t) = f_C(t)H_C + f_B(t)H_B, \quad (20)$$

where $f_C(0) = 0$, $f_B(0) > 0$, $f_C(T) > 0$, $f_B(T) = 0$, $0 \leq t \leq T$. And if the evolution is strictly adiabatic, $f_C(t)$ and $f_B(t)$ are monotonical. With the increase of t , $H(t)$ gradually changes from H_B to H_C , and $(f_C(t), f_B(t))$ completely describe the accurate process of evolution and is called adiabatic passage (AP) in this paper. The optimal adiabatic passage has the minimal evolution time T while ensuring enough fidelity (or ground state amplitude). The optimal adiabatic passage is not only monotonical, by also continuous on t .

Lemma 2. For system Hamiltonian $H(s)$, the optimal adiabatic passage $(f_C^*(t), f_B^*(t))$ are continuous.

Proof. Supposing $f_C^*(t)$ and $f_B^*(t)$ are not continuous, better adiabatic passage can be found that requires less evolution time. For example, if there exists a small interval $[t_1, t_2]$ that $f_C^*(t)$ or $f_B^*(t)$ is not continuous, $\frac{dH(t)}{dt}$ would increase significantly. During this interval, the initial and final Hamiltonian are fixed and so are the gap and eigenstate. Based on Eq. (19), here the main factor affecting the evolution time is $\frac{dH(t)}{dt}$. And if adjusting the adiabatic passage by linearly interpolating $H(t_1)$ to $H(t_2)$, $\frac{dH(t)}{dt}$ would reduce and less evolution time is required. It is a better adiabatic passage and this goes against the prerequisites of optimality. \square

To simulate the optimal evolution, the optimal adiabatic passage should be discretized as p intervals. Suppose the discretization is optimal that p is the least required depth to maintain the performance of

evolution. For the d -th interval $[t_{d-1}, t_d)$, the evolution is approximately

$$e^{if_C^*(t_d)\Delta t_d H_C} e^{if_B^*(t_d)\Delta t_d H_B}, \quad (21)$$

where $\Delta t_d = t_d - t_{d-1}$. However, when dealing a specific problem, $f_C^*(t)$ and $f_B^*(t)$ are unknown. Therefore, QAOA adopts parameters $\gamma_d = f_C(t_d)\Delta t_d$ and $\beta_d = f_B(t_d)\Delta t_d$, and simulates this evolution by variation and optimization. If there is no information about $f_C^*(t)$ and $f_B^*(t)$, this simple parameteration is the best. But the optimal adiabatic passage is known to be continuous and if regardless of the non-adiabatic process, also monotonical. And these properties would help to better parameterize $f_C(t)$ and $f_B(t)$.

There are three explicit factors in the evolution of Eq. (21), Δt_d , $f_C^*(t_d)$ and $f_B^*(t_d)$. And the relationship between these three factors is determined by the of optimality of $f_C^*(t)$ and $f_B^*(t)$, therefore,

$$\Delta t_d \sim \varepsilon(t_d)g^{-2}(t_d). \quad (22)$$

Based the Eq. (18), the main factor in $\varepsilon(t_d)$ influencing Δt_d is $\frac{dH(t)}{dt}$. Therefore, it is $(\Delta f_C^*(t_d), \Delta f_B^*(t_d))$ that directly affects Δt_d other than $(f_C^*(t_d), f_B^*(t_d))$. Here to keep the factor to be positive, $\Delta f_C^*(t_d) = f_C^*(t_d) - f_C^*(t_{d-1})$ and $\Delta f_B^*(t_d) = f_B^*(t_{d-1}) - f_B^*(t_d)$. And there are actually four internally related factors, namely, Δt_d , $g(t_d)$, $\Delta f_C^*(t_d)$ and $\Delta f_B^*(t_d)$.

Because the gap $g(t)$ is the property of Hamiltonian and cannot be adjusted by parameter, it can be regarded as independent variable. The other three factor depend on $g(t_d)$ and have different continuity. In fact, discrete variables have no continuity in the strict sense, the better continuity here refers to smaller changes of the corresponding factors between adjacent interval. Based on Eq. (22), $\Delta f_C^*(t_d)$ and $\Delta f_B^*(t_d)$ should be quadratically positively correlated to $g(t_d)$, while Δt_d is quadratically inversely related to $g(t_d)$.

The continuity of parameter helps in parameter adjusting, so the parameterization of the optimal adiabatic passage should maintain the best continuity of these factors. Obviously, $\Delta f_C^*(t_d)$ has better continuity comparing to the accumulation $f_C^*(t_d) = \sum_{j=1}^d \Delta f_C^*(t_j)$. Therefore, a straightforward consideration is directly adopting these three dependent factors as parameters, and its mapping with (γ, β) can be written as

$$\gamma_d = \sum_{j=1}^d \Delta f_C^*(t_j)\Delta t_d, \beta_d = \sum_{j=d}^p \Delta f_B^*(t_j)\Delta t_d. \quad (23)$$

Based on Section 2 and Section 3.1, with the normalized Hamiltonian, $\Delta f_C^*(t_d)$ and $\Delta f_B^*(t_d)$ should have similar property like f_γ and f_β . Therefore, $(\Delta f_C^*(t_d), \Delta f_B^*(t_d))$ can be mapped as $(\rho_d \sin \theta_d, \rho_d \cos \theta_d)$. θ_d shows the intensity ratio between H_C and H_B in ΔH_d and has an approximate expectation $\pi/4$ if the Hamiltonian is properly normalized. And it certainly has good continuity. ρ_d inherits the continuity of $\Delta f_C^*(t_d)$ and $\Delta f_B^*(t_d)$, and is positive correlated to $g(t_d)$. ρ_d shows the intensity of ΔH_d in the d -th interval and should have better continuity than $\Delta f_C^*(t_d)$ or $\Delta f_B^*(t_d)$ alone.

ρ_d , Δt_d and an extra factor p can be combined to a single parameters τ_d with better continuity, and the parameter mapping can be written as

$$\gamma_d = \frac{\sum_{i=1}^d \rho_i \sin \theta_i}{p\rho_d \sin \theta_d} \tau_d \sin \theta_d, \beta_d = \frac{\sum_{i=d}^p \rho_i \cos \theta_i}{p\rho_d \cos \theta_d} \tau_d \cos \theta_d \quad (24)$$

The analysis is as follows. ρ_d and Δt_d has opposite correlation on $g(t_d)$, so $\rho_d \Delta t_d$ has better continuity. Actually, because of the optimality of discretization, Δt_d should not be too large, and $\rho_d \Delta t_d$ is still slightly related to $g(t_d)$. On the other hand, $\sum_{d=1}^p \Delta t_d = T$, so Δt_d is actually approximately inversely proportional to p if fixing T and combining p can further improve continuity of τ .

The 3-parameter space actually works, but it would increase the complexity of parameter optimization and an approximation can be made as follows. Considering the form of $\sum_{i=1}^d \rho_i \sin \theta_i / p\rho_d \sin \theta_d$ in Eq. (24), $\rho_i \sin \theta_i$ of each layer can be approximately regard as i.i.d. random variable. With the increase of d , a linear increase would gradually dominate. Therefore, it is intuitive to extract the linear factors as $d/(p+1)$ and approximately divide the other terms with lower order into intensity effects and angle effects, and merge

them into τ_d and θ_d , respectively. Here $p + 1$ is used to avoid the bound condition when parameters become invalid. As a result, the parameter space is reduced to $(\boldsymbol{\theta}, \boldsymbol{\tau})$ and its mapping with $(\boldsymbol{\gamma}, \boldsymbol{\beta})$ is

$$\gamma_d = \frac{d}{p+1} \tau_d \sin \theta_d, \beta_d = \frac{p+1-d}{p+1} \tau_d \cos \theta_d. \quad (25)$$

This parameterization of adiabatic passage has better continuity and interpretability, and to reduce the optimization cost, the continuity should be fully utilized in parameter adjusting. Here a parameter setting method is proposed based on the continuity of adiabatic passage, as shown in Algorithm 2.

Algorithm 2 AP-based parameter setting method

Require:

- Approximately normalized Hamiltonian \bar{H}_C and \bar{H}_B and the depth of QAOA p ;
- Initial parameters $(\theta_0 = \pi/4, \tau_0 = \sqrt{2}t_0)$, where t_0 is given by Algorithm 1;
- Routine $Interp(\boldsymbol{v}, n)$ that interpolates vector \boldsymbol{v} to length of n ;

Ensure:

- The optimized parameters $(\boldsymbol{\theta}, \boldsymbol{\tau})$ for every depth of QAOA;
 - 1. Optimize θ_0 and τ_0 by the QAA-inspired adjusting method and obtain θ_0^* and τ_0^* ;
 - 2. $\bar{H}_C \leftarrow \sqrt{2}\tau_0^* \sin \theta_0^* \bar{H}_C$, $\bar{H}_B \leftarrow \sqrt{2}\tau_0^* \cos \theta_0^* \bar{H}_B$, $T_u \leftarrow \lfloor \log_2 p \rfloor$, and initialize $\boldsymbol{\theta} \leftarrow (\pi/4)$, $\boldsymbol{\tau} \leftarrow (1)$;
 - 3. If $T_u \leq 0$, finishes, otherwise, $T_u \leftarrow T_u - 1$, $\boldsymbol{\theta} \leftarrow Interp(\boldsymbol{\theta}, \lceil p/2^{T_u} \rceil)$, $\boldsymbol{\tau} \leftarrow Interp(\boldsymbol{\tau}, \lceil p/2^{T_u} \rceil)$;
 - 4. $\boldsymbol{\theta}' \leftarrow Interp(\boldsymbol{\theta}, p)$, $\boldsymbol{\tau}' \leftarrow Interp(\boldsymbol{\tau}, p)$, optimize $\langle \boldsymbol{\theta}', \boldsymbol{\tau}' | H_C | \boldsymbol{\theta}', \boldsymbol{\tau}' \rangle$ by adjusting $\boldsymbol{\theta}$ and $\boldsymbol{\tau}$, turn to 3.
-

In Require 1 and 2, this algorithm inherits Algorithm 1 that normalizes the Hamiltonian and uses an empirical value t_0 to initialize parameters, but differently, this algorithm optimize all these $2p$ parameters. In Require 3 of Algorithm 2, the interpolation function can be flexible and in simulation, cubic spline interpolation is used. Explanation of each step is as follows:

- The Step 1 applies the QAA-inspired parameter adjusting method and obtained parameters (ρ_0^*, τ_0^*) . An empirical t_0 is adopted and the method would start with good performance, but the optimization cost with initialization $(\pi/4, \sqrt{2}t_0)$ is approximately the same with that of $(\pi/4, \sqrt{2})$.
- The Step 2 normalizes the magnitude of parameter spaces in two aspects. One is fixing the approximate normalization of Hamiltonian by θ_0^* so that the initial $\boldsymbol{\theta}$ can be set as $(\pi/4)$. As for the other, noting that when adjusting θ , $\Delta\theta$ mean an increment of $\tau \sin \Delta\theta \approx \tau \Delta\theta$, Step 2 deals this unbalanced increment by mapping with τ_0^* that the initial $\boldsymbol{\tau}$ is set as (1) . Therefore, τ_d during the optimization should be $\Theta(1)$ and the increment when adjusting θ should be $\Theta(\Delta\theta)$
- T_u is an indicator and in Step 3, it is checked to approximately double the dimension of parameter space of $(\boldsymbol{\theta}, \boldsymbol{\tau})$ by interpolation. Until the dimension is full and optimized, algorithm terminants.
- The Step 4 interpolates the limited-dimensional parameters to full dimension of $(\boldsymbol{\theta}', \boldsymbol{\tau}')$ and optimizes the expectation $\langle \boldsymbol{\theta}', \boldsymbol{\tau}' | H_C | \boldsymbol{\theta}', \boldsymbol{\tau}' \rangle$, where $|\boldsymbol{\theta}', \boldsymbol{\tau}' \rangle$ is the quantum state after evolution with parameters $(\boldsymbol{\theta}', \boldsymbol{\tau}')$. Pay attention that during optimization, only $(\boldsymbol{\theta}, \boldsymbol{\tau})$ are adjusted.

In this method, there are mainly two essential points to reduce the optimization cost. One is the reuse of parameters. The optimized $(\boldsymbol{\theta}, \boldsymbol{\tau})$ of any dimension is a kind of estimation of optimal adiabatic passage. Therefore, with the optimized $(\boldsymbol{\theta}, \boldsymbol{\tau})$ of dimension l_1 , a good initialization of $(\boldsymbol{\theta}, \boldsymbol{\tau})$ of dimension l_2 can be simply obtained by interpolation. Here the interpolation can be replaced by other algorithm like Fourier transform as long as the continuity is involved. Another is the normalization. The normalization of Hamiltonian reduces the impact of problem on parameters, specifically for $F_s(n, m, 3)$, the m . And the mapping of \bar{H}_C and \bar{H}_B in Step 2 not only fixes the approximate normalization by θ_0^* , but also eliminates the impact of the scale n by τ_0^* with consideration to the practical meaning of τ . That is, the magnitude of parameter is completely separated the problem.

Table 1: The average expectation of QAA-inspired adjusting method and INTERP heuristic with error bar of 95% confidence.

Scale (n)	13	14	15	16	17	18	19	20
QAA-inspired	0.985 ± 0.014	0.986 ± 0.012	0.987 ± 0.011	0.987 ± 0.010	0.987 ± 0.011	0.988 ± 0.009	0.989 ± 0.008	0.989 ± 0.009
INTERP	0.941 ± 0.010	0.941 ± 0.009	0.941 ± 0.009	0.941 ± 0.011	0.940 ± 0.009	0.940 ± 0.008	0.940 ± 0.009	0.940 ± 0.009

4 Comparison and performance

Some details of simulation in this section are displayed here. First, the evaluation. Generally, the performance of QAOA can be evaluated by the expectation, but based on the reduction in Lemma 1, the algorithm only succeeds when the target is obtained, that is, only the probability of target state is concerned. As for the parameter setting method, another evaluation of performance is the optimization cost, that is, the required number of runs of the quantum circuit. Second, the optimization aim. As the algorithm should terminate as long as the target is found, the expectation is still used to adjust parameters. Third, the problem set. The instances used in simulation is generated by random model $F_s(n, m, 3)$ and the scale n would be given in simulation. Actually, the difficulty of 3-SAT also changes with m . And in this paper, m is fixed as an experimental m_n^* that the average success probability of $F_s(n, m_n^*, 3)$ is generally small comparing to other m when applying the QAA-inspired adjusting method. That is, a statistical hard problem set of random 3-SAT. In simulation, $m_n^* = \tilde{\mu}_n n$, where $\tilde{\mu}_n$ slightly increases with n from 5.9 to 6.3 when $10 \leq n \leq 20$. Fourth, the classical optimization routine. Although the performance of these methods proposed in this paper are nearly not correlated with the classical optimization routine, for convenience of comparison, a gradient-based optimization routine (BFGS) is used corresponding to [32].

4.1 Comparison

This subsection compares the performance of the methods in this paper with the heuristic strategies proposed in [32] and further displays the performance on more general instances. In [32], two kind of heuristic strategies are proposed, the INTERP heuristic and the FOURIER heuristic, and the FOURIER heuristic strategy is one of the most widely used high-efficient method for parameter setting of QAOA.

4.1.1 Comparison of QAA-inspired parameter initialization with INTERP heuristic

This QAA-inspired parameter initialization can be modified to a two-parameter setting method of (θ, ρ) for QAOA and the resulted (γ, β) follows a linear variation. This is similar with that of INTERP heuristic which also follows a linearly-variant parameters and therefore, only two adjustable parameters. The specific steps of INTERP heuristic is as follows:

- (1) QAOA starts from depth of $p_t = 1$ and randomly initializes the parameters γ_0, β_0 .
- (2) The parameters $(\vec{\gamma}, \vec{\beta})$ of length p_t are obtained through linear interpolation of (γ_0, β_0) , that is, $\gamma_d = d\gamma/(p_t + 1)$, $\beta_d = (p_t + 1 - d)\beta/(p_t + 1)$, optimize the expectation by adjusting γ_0, β_0 .
- (3) If $p_t \geq p$, terminate, otherwise set $p_t \leftarrow p_t + 1$, jump to Step 2.

The QAA-like parameter initialization method is based on the problem model of random 3-SAT and normalizes the Hamiltonian. As a result, a feasible initialization can be obtained as $(\theta = \pi/4, \rho = \sqrt{2})$ and the circuit can start with full depth of p . While for the INTERP heuristic, it is general and disregards the problem model. Therefore, there is no knowledge about the problem, and the circuit can only start with a small depth and gradually increase the depth until p . Comparative simulation is conducted for these two methods on random instances in $F_s(n, m, 3)$ and the performance is evaluated by optimization cost and the probability of aimed state, as presented in Figure 7 and 8. In order not to cause misunderstanding about performance, the average expectations are also simply displayed in Table 1.

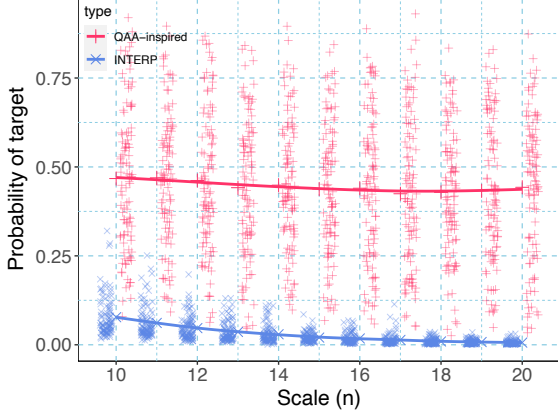


Figure 7: The distribution of probability of target state for instances in $F_s(n, m, 3)$. The result of QAA-inspired adjusting method is plotted in red, the raw data in red plus sign in the right side and the average is smoothed in red line. While the INTERP heuristic is plotted in blue, the raw data in blue cross in the left side and the average smoothing in blue line.

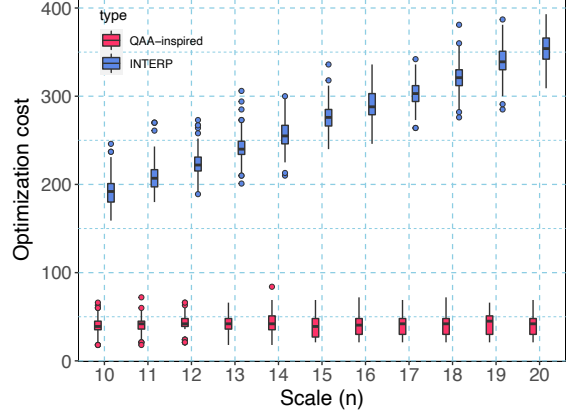


Figure 8: The distribution of the optimization cost for $F_s(n, m, 3)$ plotted in box plot. The result of QAA-inspired adjusting method is plotted in red in left side and the INTERP heuristic is plotted in blue in right side. The result shows that the cost for QAA-based is generally constant on n , while the INTERP heuristic keeps a linear increasing.

The performance of QAA-inspired parameter optimization method is much better than that of INTERP heuristic, and this significant difference in performance mainly stems from following two reasons. The first is the normalization of the Hamiltonian, and its impact on performance is the probability. When the Hamiltonian is not normalized, it is difficult to find a suitable initialization. This is reflected in the phenomenon that the performance of INTERP is highly dependent on the initial point. In [32], because the simulation is done on max-cut, the intensity difference between H_C and H_B is not huge, so the decline in performance is not obvious. Besides, in simulation of [32], multiple repetitions might be conducted when depth $p_t = 1$ to find a good initialization, but here only one try is proceeded for both method. The other is the mapping of parameter space, and it mainly influences the optimization cost. Because ρ extracts the intensity of parameters γ and β , θ is close to the optimum and during optimization, ρ is mainly adjusted. The INTERP knows little about the parameter space and has to optimize from $p_t = 1$ to $p_t = p$, so the linear factor appears. While the QAA-inspired method has good explainable initializations and with only two parameters in one optimization loop, constant cost is obvious.

4.1.2 Comparison of AP-based parameter setting with FOURIER heuristic

The AP-based parameter setting method optimizes all these $2p$ parameters and has similarity with FOURIER heuristic that try to reduce the optimization cost by utilizing the continuity of parameters. Besides, the FOURIER heuristic strategy introduces another parameter q to restrict the degree of freedom of parameter space, while the AP-based method also uses an indicator T_u to control the degree of freedom. Both methods can terminate with an insufficient optimization, but here to compare the performance, the full parameter space is optimized. The steps of FOURIER in this situation is presented as follows:

- (1) QAOA starts from depth of $p_t = 1$ and randomly initializes the parameters $\vec{u} = (u_1), \vec{v} = (v_1)$.
- (2) Obtain $(\vec{\gamma}, \vec{\beta})$ by transform $\gamma_i = \sum_k u_k \sin((k - \frac{1}{2})(i - \frac{1}{2})\pi/p_t)$, $\beta_i = \sum_k v_k \cos((k - \frac{1}{2})(i - \frac{1}{2})\pi/p_t)$, and optimize the expectation of QAOA with depth p_t by adjusting (\vec{u}, \vec{v}) .

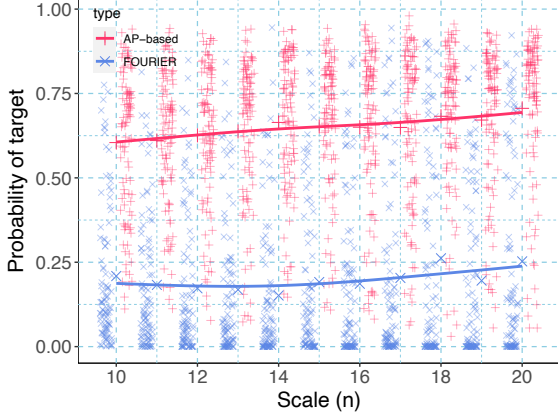


Figure 9: The distribution of probability of target state on instances in $F_s(n, m, 3)$. The result of AP-based optimization method is plotted in red, the raw data in red plus sign of right side and the average is smoothed in red line. While the FOURIER heuristic is plotted in blue, the raw data in blue cross of left side and the average smoothing in blue line.

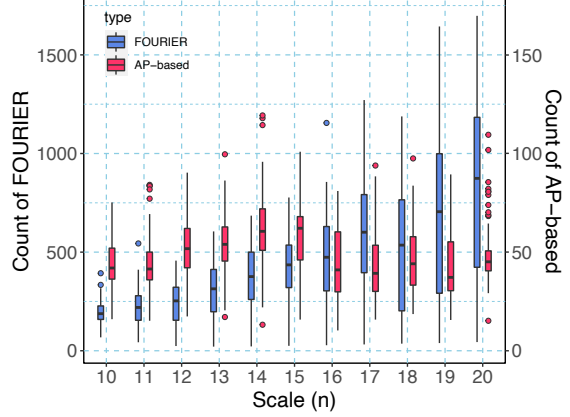


Figure 10: The distribution of the optimization cost for $F_s(n, m, 3)$ plotted in box plot. The result of AP-based optimization method is plotted in red and the FOURIER heuristic is plotted in blue. Because of the difference in degree of amplitude for both result, dual y-axis is used to display the change of the cost more clearly.

- (3) If $p_t \geq p$, terminate, otherwise set $p_t \leftarrow p_t + 1$, expand parameters $\vec{u} \leftarrow (u_1, \dots, u_{p_t}, 0)$, $\vec{v} \leftarrow (v_1, \dots, v_{p_t}, 0)$, and jump to Step 2.

Like the INTERP, FOURIER does not consider model of problem and the circuit start with a small depth, while the AP-based method inherits the advantage of QAA-inspired method and starts with a good initialization with full depth of p . Furthermore, the AP-based method reforms the parameter space of (γ, β) to another with better continuity. Comparative simulation is conducted for these two method on random instances in $F_s(n, m, 3)$ and the performance is presented in Figure 9 and 10.

Comparing with the performance of INTERP, the FOURIER shows better performance on probability of target state although without Hamiltonian normalization, but still far less than that of the QAA-inspired and AP-based method. With respect to the good performance of FOURIER on max-cut in [32], it reveals the importance of Hamiltonian normalization for the problem like 3-SAT that has problem Hamiltonian with a quickly growing intensity. Besides, in this paper, only one repetition is conducted to set the initial parameters and this also results in the poor performance of these heuristic strategies that the optimization getting stuck in a bad local optimum. In fact, with Hamiltonian normalization, FOURIER should have a similar performance on success probability comparing with the AP-based method because the computational capability of the variational quantum circuit is the same.

Another criteria to evaluate the parameter setting method is the optimization cost. Although the FOURIER heuristic method is stuck in a local optimum in simulation, it does not affect the analysis of optimization cost. Actually, the cost to arrive the global optimum is generally larger than that of local optimum. In simulation of the QAA-inspired method, the cost stays approximately constant with the increase of n , and in AP-based method, it seems sublinear and the detail would be discussed in Section 4.2. As for the FOURIER, the cost is approximately in $O(n^2)$, with average about 2000 when $n = 10$ and 8000 when $n = 20$. This magnitude derives from two factors, one from the increasing p_d like the INTERP, another is from the degree of freedom of parameters increased to p . In fact, the consideration of Sin/Cos Fourier transform to utilize the continuity of parameter is a good idea, but the continuity of (γ, β) is worse than (θ, τ) . If applying the Sin/Cos Fourier transform to parameter space (θ, τ) , the performance is at least the same with the AP-based method, and even has better performance in scenario when limiting the degree of freedom of parameters.

Table 2: The average optimization cost of the AP-based method for 1000 instances in $F_s(n, \tilde{\mu}_n n, 3)$.

Scale (n)	[4	5	6	7]	[8	9	10	11	12	13	14	15]	[16	17	18	19	20]
Average cost	300.5	342.9	379.5	410.6	430.4	440.3	445.0	446.4	532.2	544.3	586.0	612.2	524.9	535.7	549.6	512.8	540.3

4.2 Performance

4.2.1 Performance analysis

The average optimization cost of the AP-based method with $4 \leq n \leq 20$ is presented in Table 2. With the increase of n , the depth p also increases and so is the number of parameters, but the cost does not remain strictly increasing. First of all, the increase obviously slower than linear, from 300.4 when $n = 4$ to 540.3 when $n = 20$. To be precise, it seems to grow within certain interval but also fluctuate when acrossing certain value. In the AP-based method, the procedure of parameter interpolation is divided into $l = \lfloor \log_2 p \rfloor$ parts and for each part, the degree of freedom is (approximately) doubled. And noting that in Table 2, a significant drop is around $n = 16$, where the continuity between parameters before and after interpolation is best. In fact, the range of cost can be divided by n into three intervals, $4 \leq n \leq 7$, $8 \leq n \leq 15$ and $16 \leq n \leq 20$. In each interval, l is the same, but the number of parameters increases. Therefore, the continuity of interpolation decreases and as a result, the cost increases. And the most representative results should be the cost when $n = 2^l$. When $l = 2, 3, 4$, the average costs are 300.5, 430.4 and 524.9, approximately $O(l)$. This reveals that in this limited simulation, the optimization cost might be $O(\log(p))$.

Moreover, if considering a specific situation when $n = 16$, the optimization cost gradually increases with the decrease of T_u in Algorithm 2, that is, the increase of degree of freedom 2^{4-T_u} of the parameters. The accumulated cost for each $4 - T_u = 0, 1, 2, 3, 4$ is 40.7, 123.1, 294.7, 448.6, 524.9, respectively, and this also follows an approximately linear increasing. Besides, this result is rather similar to the full cost when $n = 2^l$ with $l = 2, 3, 4$, and this reveals two points. Firstly, the optimization cost of this method is nearly not correlated with n or p , but the degree of freedom of parameters. Secondly, the logarithmic factor of optimization cost might stems from the logarithmic increasing loop when interpolating parameters.

To show the continuity of optimal parameters, the optimized parameters of five examples are plotted in Figure 11. These optimized parameters shows nice continuity that it follows a form similar to that of trigonometric functions, and the centralization of θ_d and ρ_d is actually around $\pi/4$ and 1. In simulation, the impact of the variation of $g(s)$ is significantly reduced that $\max_d\{\tau_d\}$ is no more than twice as much as $\min_d\{\tau_d\}$. But for $g(s)$, the maximum differs much with the minimum. This result coincidents with the analysis of the normalization of the Hamiltonian and the continuity of parameters in Section 3. Furthermore, it reveals that the Sin/Cos Fourier transform should be better to utilize the continuity between parameters. The paper applies the interpolation only because of its simplicity.

4.2.2 Performance on general instances

Simulation is conducted on 100,000 random instances in $F_s(n, m, 3)$ for each scale $10 \leq n \leq 20$. To show the initial capability of the QAA-inspired parameter initialization method, a empirical t_0 is given but without any parameter adjusting. Besides, for comparison, not only 3-SAT with $m = \tilde{\mu}_n n$, but also instances $m = n^2$ are considered. The distribution of probability of target state is presented in Figure 12. When $m = n^2$, the success probability is rather large and the average significantly increases with n . As for the harder situation when $m = \tilde{\mu}_n n$, the median of success probability generally keeps stable around 0.43 and it implies that the most instances can be dealled within several runs of circuit. In the other hand, there are still some hard instances with small probability and when $n = 20$, 1% instances has success probability less than 0.0422.

Another simulation is conducted on these 1% hardest instances and the AP-based parameter setting method is applied to optimize the parameters. The distribution of probability before and after optimization is presented in Figure 13. With only initial parameters, the success probability are all lower than 0.05, and after optimization, the overall probability significantly increases and can be boost over 0.2 for some instances. On the other hand, the count of instances with success probability lower than 0.001 keeps invariant. These

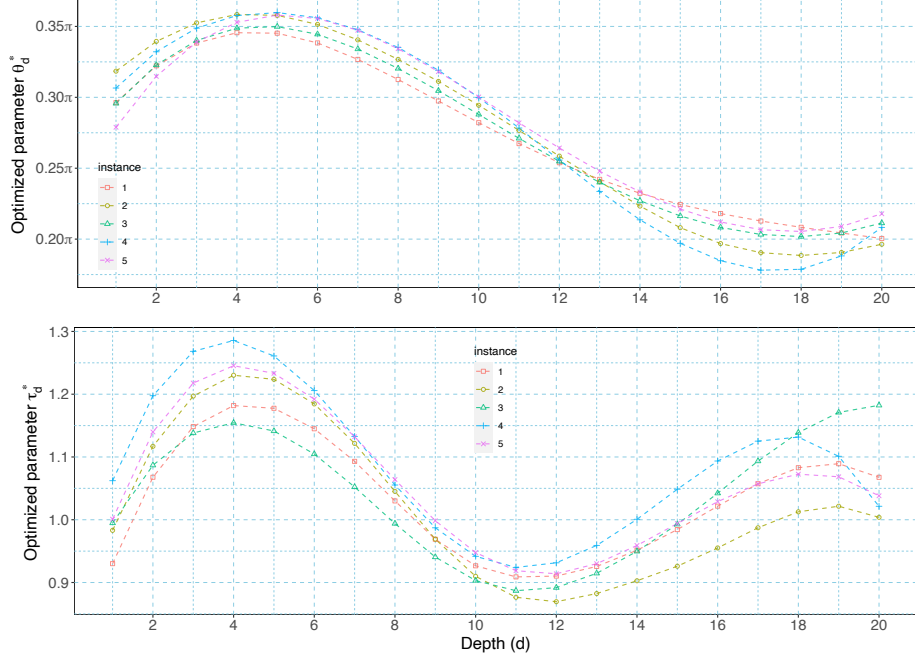


Figure 11: The distribution of optimized paramters θ^* and τ^* for five different instances in $F_s(20, m, 3)$. Parameters of each instance are plotted in different color and shape, and the adjacent points are connected directly using straight lines. These polylines form a fitting of a curve similar to a trigonometric function.

Table 3: The average required run times of circuit when applying the AP-based method for 100,000 instances in $F_s(n, \tilde{\mu}_n n, 3)$.

Scale (n)	10	11	12	13	14	15	16	17	18	19	20
Average runs	2.978	3.161	3.213	3.308	3.461	3.499	3.443	3.565	3.655	3.753	4.087

critical hard instances can has two possible classifications. One is the instance is essentially hard because of NP-completeness of 3-SAT, another is the real G_0 of the instances differs much from the estimation G_E and the optimization is stuck in a bad local optimum. The latter can be dealt to some extent by more attention of G_E , but the optimization cost would increase. Luckily, the frequency of this kind of instances is small enough, 7 in 100,000 and there is no instance with probability less than 0.01%. This frequency is far larger than probability of 0.01%, and if considering $n = 20$, it can be exponentially small and the average cost for $F_s(n, m, 3)$ is still acceptable.

The actual required runs of quantum circuit is different to that when optimizing the parameters. In application, the method can terminate in any step as long as the solution is obtained. And when adjusting parameter, circuit need multiple runs (generally 100 to 1000) to obtain the expectation and here fixes 100 runs. Modifying Algorithm 2 to terminate when obtaining the solution, simulation is conducted these 100,000 instances in $F_s(n, \tilde{\mu}_n n, 3)$ with $10 \leq n \leq 20$. And the average runs of quantum circuit is presented in Table 3. This performance is attributed to the good parameter intialization method and with only several runs of circuit, the result can be obtained. Different to the average probability, average runs gradually increases sublinearly and this increment stems from these hard instances. But the average complexity is acceptable. The complexity of a single run of quantum circuit is determined by H_C and the depth p , namely, $O(mp)$.

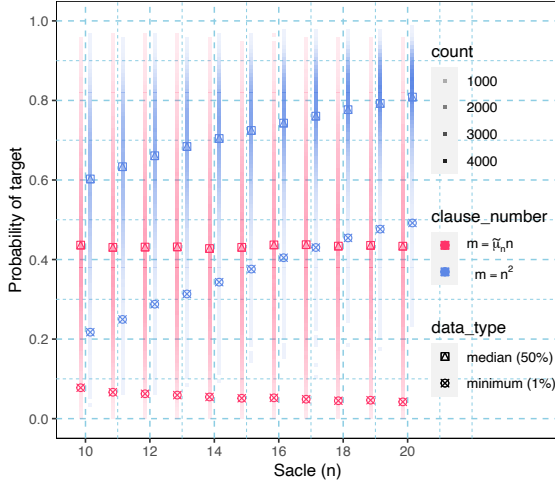


Figure 12: The distribution of success probability for 1000,000 instances of $F_s(n, m, 3)$ with initial parameters, where $10 \leq n \leq 20$. The left red points represents for $m = \tilde{\mu}_n n$ and the right blue points for $m = n^2$, and the shades of color represent the count. The median (50%) of probability is plotted in square-triangle points and the minimal 1% is in round-cross.

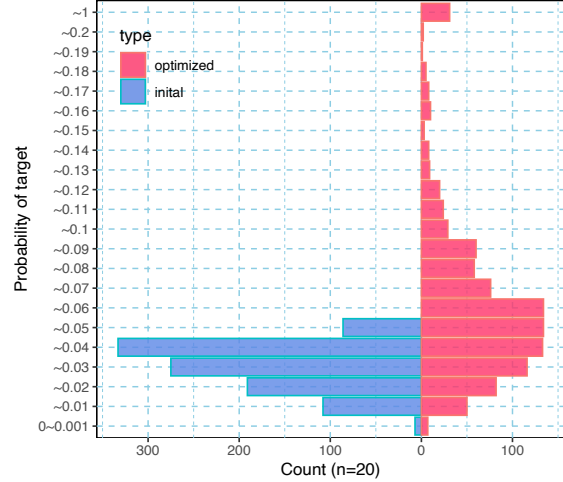


Figure 13: The distribution of success probability for these 1000 harder instances of $F_s(20, \tilde{\mu}_n n, 3)$. The blue column in the left shows the success probability with only initial parameters and the red column in the right shows the optimized. For probability over 0.2 or below 0.001, the results are presented in a single column, and the counts are 31 and 7, respectively.

5 Conclusion and outlook

This paper discusses the details of QAOA on 3-SAT problem and provides an efficient parameter setting method. There are two main points. One is the preprocessing based on the problem model that normalizes the Hamiltonian. And based on this, a QAA-inspired parameter initialization method is introduced. The other is the adjustment of parameter space. Based on the analysis of the continuity between parameters, the (γ, β) parameter space is transformed into (θ, τ) with better continuity. Correspondingly, a parameter setting method based on continuity is proposed.

In fact, although the analysis and simulation in this paper are based on the k-SAT model, the framework of this method is universal. For other combinatorial optimization problem like max-cut and max-clique, the random model can also be established that each instance is randomly and uniformly generated. And based on this, the random Hamiltonian of this model can be built. Here, in order to make the Hamiltonian easier to analyze, there are a lot remains to research, including but not limited to problem reduction, model approximation, etc. Then, according to the statistical properties of the random Hamiltonian, the estimation of the maximum energy difference of H_C can be estimated, and the parameter setting method in the paper can be applied.

This framework of parameter-setting for QAOA has several advantages. Firstly, the good initialization for full depth of QAOA means good computational ability as the start of algorithm, other than gradually increasing depth and adjusting parameters. Secondly, the parameter settings are separated from the overall property of the problem, and this keeps the magnitude of parameters to be the same for different instances. Thirdly, this parameterization of adiabatic passage not only provides better continuity between parameters, but also provide good interpretability for parameters setting and it would be help for understanding and further research.

There is still rooms of improvement for this method in two aspects. One is the continuity. There might be another parameterization for the optimal adiabatic passage, and other method to replace interpolation,

like the Sin/Cos Fourier transform. The other is the non-adiabatic process. The analysis in the paper mainly considers the adiabatic process, but the circuit of QAOA can also simulate the non-adiabatic process and in some situations, has better performance. Actually, this parameterization works on non-adiabatic process, but the interpretability becomes poor. Furthermore, there are still some remaining work beyond this method. Firstly, further discussion about the average complexity of random 3-SAT can be conducted based on this method and analysis in this paper. Secondly, more applications can be conducted on problems that not only limited to combinatorial optimization.

References

- [1] Nielsen M A, Chuang I L. Quantum Computation and Quantum Information. Cambridge: Cambridge University Press, 2000
- [2] Shor P W. Polynomial-time algorithms for prime factorization and discrete logarithms on a quantum computer. *SIAM Rev*, 1999, 41: 303–332
- [3] Grover L K. Quantum Mechanics Helps in Searching for a Needle in a Haystack. *Physical Review Letters*, 1997, 79: 2
- [4] Harrow A W, Hassidim A, Lloyd S. Quantum algorithm for linear systems of equations. *Phys Rev Lett*, 2009, 103: 150502
- [5] Preskill J. Quantum Computing in the NISQ era and beyond. *Quantum*, 2018, 2: 79
- [6] Cerezo M, Arrasmith A, Babbush R. Variational quantum algorithms. *Nature Reviews Physics*, 2021, 3: 9(625–644)
- [7] Biamonte J, Wittek P, Pancotti N. Quantum machine learning. *Nature*, 2017, 549(7671):195?202
- [8] Farhi E, Neven H. Classification with quantum neural networks on near term processors. 2018. arXiv:1802.06002.
- [9] Peruzzo A, Jarrod M, Shadbolt P, et al. A variational eigenvalue solver on a photonic quantum processor. *Nature Communications*, 2014, 5: 1(4213)
- [10] Kandala A, Mezzacapo A, Temme K. Hardware-efficient variational quantum eigensolver for small molecules and quantum magnets. *Nature*, 2017, 549: 7671(242–246)
- [11] Farhi E, Goldstone J, Gutmann S. A Quantum Approximate Optimization Algorithm. 2014. ArXiv: 1411.4028
- [12] Moll N, Barkoutsos P, Bishop L S, et al. Quantum optimization using variational algorithms on near-term quantum devices. *Quantum Science and Technology*, 2018, 3: 3(030503)
- [13] Harrigan M P, Sung K J, Neeley M, et al. Quantum approximate optimization of non-planar graph problems on a planar superconducting processor. *Nature Physics*, 2021, 17: 3(332–336)
- [14] Jiang Z, Rieffel E G, Wang Z. Near-optimal quantum circuit for Grover’s unstructured search using a transverse field. *Phys Rev A*, 2017, 95: 6
- [15] Wang Z, Hadfield S, Jiang Z, et al. Quantum approximate optimization algorithm for MaxCut: A fermionic view. *Phys Rev A*, 2018, 97: 2
- [16] Basso J, Farhi E, Marwaha K, et al. The Quantum Approximate Optimization Algorithm at High Depth for MaxCut on Large-Girth Regular Graphs and the Sherrington-Kirkpatrick Model. 2021. ArXiv: 2110.14206

- [17] Farhi E, Goldstone J, Gutmann S, et al. The Quantum Approximate Optimization Algorithm and the Sherrington-Kirkpatrick Model at Infinite Size. 2021. ArXiv: 1910.08187
- [18] Brandao F G.S.L, Broughton M, Farhi E, et al. For Fixed Control Parameters the Quantum Approximate Optimization Algorithm’s Objective Function Value Concentrates for Typical Instances. 2018. ArXiv: 1812.04170
- [19] Farhi E, Harrow A W. Quantum Supremacy through the Quantum Approximate Optimization Algorithm. 2019. ArXiv: 1602.07674
- [20] Barak B, Marwaha K. Classical algorithms and quantum limitations for maximum cut on high-girth graphs. 2021. ArXiv: 2106.05900
- [21] Streif M, Yarkoni S, Skolik A, et al. Beating classical heuristics for the binary paint shop problem with the quantum approximate optimization algorithm. *Physical Review A*, 2018, 104: 1
- [22] Wang Z., Rubin N. C., Dominy J. M., et al. XY mixers: Analytical and numerical results for the quantum alternating operator ansatz. *Physical Review A*, 2020, 101: 1 (012320)
- [23] Bakó B, Glos A, Salehi ö, et al. Near-optimal circuit design for variational quantum optimization. 2022. ArXiv: 2209.03386
- [24] Ruan Y, Yuan Z, Xue X, et a. Quantum approximate optimization for combinatorial problems with constraints. *Information Sciences*, 2023, 619: 98-125
- [25] Farhi E, Goldstone J, Gutmann S, et al. Quantum Computation by Adiabatic Evolution. 2000. ArXiv: 0001106
- [26] Farhi E, Goldstone J, Gutmann S, et al. A Quantum Adiabatic Evolution Algorithm Applied to Random Instances of an NP-Complete Problem. *Science*, 2001, 292: 5516(472–475)
- [27] Crooks G E. Performance of the Quantum Approximate Optimization Algorithm on the Maximum Cut Problem. 2018. ArXiv: 1811.08419
- [28] Verdon G, Broughton M, McClean J R, et al. Learning to learn with quantum neural networks via classical neural networks. 2019. ArXiv: 1907.05415
- [29] Jain N, Coyle B, Kashefi E, et al. Graph neural network initialisation of quantum approximate optimisation, *Quantum*, 2022, 6: 861.
- [30] Moussa C, Wang H, Bačk T, and V. Dunjko, Unsupervised strategies for identifying optimal parameters in Quantum Approximate Optimization Algorithm, *EPJ Quantum Technology* 9, 11 (2022)
- [31] Streif M, Leib M. Training the quantum approximate optimization algorithm without access to a quantum processing unit. *Quantum Sci Technol*, 2020, 5: 3
- [32] Zhou L, Wang S, Choi S, et al. Quantum Approximate Optimization Algorithm: Performance, Mechanism, and Implementation on Near-Term Devices. *Phys Rev X*, 2020, 10: 2
- [33] Wurtz J, D. Lykov, Fixed-angle conjectures for the quantum approximate optimization algorithm on regular MaxCut graphs, *Phys. Rev. A*, 2021, 104: 052419
- [34] Egger D J, Mareček J, Woerner S. Warm-starting quantum optimization, *Quantum*, 2021, 5: 479
- [35] Tate R, Farhadi M, Herold C, et al. Bridging Classical and Quantum with SDP initialized warm-starts for QAOA, *ACM Transactions on Quantum Computing* 2023, 4, 1.
- [36] Boulebnane S, Montanaro A. Predicting parameters for the Quantum Approximate Optimization Algorithm for MAX-CUT from the infinite-size limit. 2021. ArXiv: 2110.10685

- [37] Achlioptas D, Moore C. Random k-SAT: Two Moments Suffice to Cross a Sharp Threshold. *SIAM Journal on Computing*, 2006. 36: 3(740–762)
- [38] Korte B, Vygen J, Korte B, et al. *Combinatorial optimization*, Springer, 2012, Vol. 2
- [39] Welch J, Greenbaum D, Mostame S, et al. Efficient quantum circuits for diagonal unitaries without ancillas. *New Journal of Physics*, 2014, 16: 3
- [40] Andrew L. Ising formulations of many NP problems. *Frontiers Media SA*, 2014, 2
- [41] Barenco A, Bennett C H, Cleve R, et al. Elementary gates for quantum computation. *Phys Rev A*, 1995, 52: 5(3457–3467)
- [42] Albash T, Lidar D A. Adiabatic quantum computation. *Review of Modern Physics*, 2018, 90: 015002
- [43] Farhi E, Gamarnik D, Gutmann S. The Quantum Approximate Optimization Algorithm Needs to See the Whole Graph: A Typical Case. 2020. *ArXiv: 2004.09002*